Understanding the effect of host flexibility on the adsorption of CH_4, CO_2 and SF_6 in porous organic cages

Siyuan Yang[a,b], Linjiang Chen[b,c], Daniel Holden[b], Ruiyao Wang[a], Yuanyuan Cheng[d], Mona Wells[e], Andrew I. Cooper[b,c], and Lifeng Ding*[a]*

a Department of Chemistry, Xi'an JiaoTong-Liverpool University, 111 Ren'ai Road, Suzhou Dushu Lake Higher Education Town, Jiangsu Province, 215123, China

b Department of Chemistry and Materials Innovation Factory, University of Liverpool, 51 Oxford Street, Liverpool, L7 3NY, United Kingdom

c Leverhulme Research Centre for Functional Materials Design, Materials Innovation Factory and Department of Chemistry, University of Liverpool, 51 Oxford Street, Liverpool, L7 3NY, Unite Kingdom

d School of Environmental Science & Engineering, Suzhou University of Science & Technology, Suzhou, China

e Department of Environmental Science, Xi'an JiaoTong-Liverpool University, 111 Ren'ai Road, Suzhou Dushu Lake Higher Education Town, Jiangsu Province, 215123, China

Corresponding authors: Lifeng Ding (Lifeng.Ding@xjtlu.edu.cn), Linjiang Chen (Linjiang.Chen@liverpool.ac.uk)

Keywords:

Organic molecular crystals, porous organic cages, gas adsorption, molecular simulation

ABSTRACT:

Molecular simulations for gas adsorption in microporous materials with flexible host structures is challenging and, hence, relatively rare. To date, most gas adsorption simulations have been carried out using the grand-canonical Monte Carlo (GCMC) method, which fundamentally does not allow the structural flexibility of the host to be accounted for. As a result, GCMC simulations preclude investigation into the effect of host flexibility on gas adsorption. On the other hand, approaches such as molecular dynamics (MD) that simulate the dynamic evolution of a system almost always require a fixed number of particles in the simulation box. Here we use a hybrid GCMC/MD scheme to include host flexibility in gas adsorption simulations. We study the adsorption of three gases—CH_4, CO_2, and SF_6—in the crystal of a porous organic cage (POC) molecule, CC3-R, whose structural flexibility is known by experiment to play an important role in adsorption of large guest molecules.[1,2] The results suggest that hybrid GCMC/MD simulations can reproduce experimental adsorption results, without the need to adjust the host–guest interactions in an *ad hoc* way. Negligible errors in adsorption capacity and isosteric heat are observed with the rigid-host assumption for small gas molecules such as CH_4 and CO_2 in CC3-R, but the adsorption capacity of the larger SF_6 molecule in CC3-R is hugely underestimated if flexibility is ignored. By contrast, hybrid GCMC/MD adsorption simulations of SF_6 in CC3-R can accurately reproduce experiment. This work also provides a molecular level understanding of the cooperative adsorption mechanism of SF_6 in the CC3-R molecular crystal.

INTRODUCTION

Microporous materials underpin a range of industrial gas adsorption and separation processes.[3–5] Accurate understanding of gas adsorption in microporous materials is therefore the key to the design of new materials for efficient adsorption and separation. Microporous materials such as

metal-organic frameworks (MOFs),[6] covalent-organic frameworks (COFs),[7] zeolitic imidazolate framework (ZIFs),[8] porous aromatic frameworks (PAFs)[9] and porous molecular crystals[10,11] have emerged as new adsorbents for gas adsorption and separation performances. More recently, porous molecular solids have attracted growing interest for gas adsorption and separation applications.[11–14] Unlike MOFs and COFs, which are extended framework structures, porous molecular solids are assembled by close packing of discrete molecular subunits, such as calixarenes and cage-like molecules.[15,16] Molecular crystals result from the balance of many competing, weak interactions, such as van der Waals (vdW) and electrostatic interactions. The discrete molecular subunits are not connected by strong chemical bonds, which leads to distinct properties such structural flexibility and solution processability.[17–19]

Porosity in molecular crystals that are built from porous organic cage (POC) molecules is a function of both the stability of the molecular shape and the stability of the crystal packing. Also, the extent of interconnected porosity between intrinsic pores (inside cage molecules) and extrinsic pores (in-between cage molecules) can be affected by the structural flexibility of the molecular crystal. For example, local, transient molecular flexibility might allow diffusion guest molecules that are seemingly too large into the intrinsic cage cavity,[2] while large rearrangements of the cage molecules in the solid state can give rise to "on/off" porosity switching behaviour.[17] The effects of such structural flexibility in porous molecular crystals can profoundly affect practical adsorption properties but they are still a challenge to probe and understand, both experimentally and computationally. Also, this lack of understanding thwarts the 'intuitive' structure–function relationships: for example, a cage that is designed to size-exclude a particular molecule in a separation may nonetheless adsorb that molecule due to structural flexibility.

Molecular simulations are a powerful tool for characterizing porosity in microporous materials, in principle allowing us to identify optimal structures for a target adsorption/separation application.[20,21] Most of the existing simulations of gas adsorption in microporous materials—such as MOFs, COFs, ZIFs and PAFs,[22–25] as well as porous molecular crystals[1,26]—have been carried out with the grand-canonical Monte Carlo (GCMC) method while treating the host adsorbent structures as rigid, which is referred to here as the "rigid host model". However, adsorption-induced structural changes to the host adsorbent are commonplace in various classes of microporous materials.[21,27–29] Clearly, any dynamic flexibility of the host structure cannot be accounted for by simulations based on the rigid host model, which typically uses the time- and volume-averaged crystal structure from X-ray crystallography.

Porous organic cage crystals have been the subject of several previous studies on the adsorption behaviour of flexible hosts. Chen *et al.* showed that the dynamic window apertures of a POC molecule, CC3, allowed the diffusion of gases that would otherwise be too large to pass through the static, single-crystal structure of CC3.[30] In a follow-up, computational study, it was demonstrated that the molecular flexibility of CC3 was the key to transient pore-channel formation, which would go on to influence the diffusion of gas molecules.[21] Holden *et al.* further showed that taking into account the host flexibility was essential to correctly (albeit qualitatively) explain the porosity of another POC molecule.[31] All those studies employed a combination of GCMC simulations, using a rigid host, for adsorption predictions and molecular dynamics (MD) simulations to investigate the effects of the host flexibility on the diffusion of guest molecules at pre-defined loadings. This is also common practice when studying adsorption properties of flexible framework-type materials computationally.[32,33] By contrast, adsorption simulations with a flexible host structure (termed as "flexible host model", hereafter) are rare in the literature. Thijs *et al.* included the flexibility of the zeolite silicalite in GCMC simulations by allowing the host atoms to

have translational Monte Carlo moves, thus directly investigating the influence of the framework flexibility on the adsorption of hydrocarbons.[34] Sholl *et al.* developed an alternative strategy to account for the flexibility of a MOF in adsorption predictions by running standard GCMC simulations on a series of static snapshots taken from MD simulations of the MOF performed separately.[35] It should be noted that considerable amounts of recent efforts have gone into probing and understanding guest-induced structural changes of the host structure. Wu *et al.* showed that a 2D highly flexible and breathing porous framework exhibited a double-step adsorption of CO_2, because of the structural contraction or expansion of the host framework during gas removal and uptake.[36] Meza-Morales *et al*. studied CO_2 adsorption in a coordination polymer CPL-2 experimentally and computationally, and found that rotational movements of the host ligands directly influenced the adsorption of CO_2.[37] Uncommon adsorption behaviours, such as negative gas pressures, have also been observed for CO_2 adsorption in flexible MOFs.[38] Molecular crystals have also been reported to show interesting guest-induced host structural changes. Sheng *et al*. presented a flexible molecular crystal with high adsorptive selectivity of $CHCl_3$ over ethyl acetate, facilitated by guest triggered alkyl transformation.[39] Nikolayenko *et al*. demonstrated a structurally dynamic and robust halogen-bonded molecular crystal that underwent reversible switching of its pore volume by exposure to different gases of different sizes and shapes.[40]

In this work, we use a hybrid GCMC/MD scheme, which allows for direct sampling of host motions in adsorption simulations, to study the gas adsorption of CH_4, CO_2 and SF_6 in a porous organic cage crystal, CC3-R.[16] The CC3-R cage molecule has an internal void of 80 $Å^3$, which is accessed through the four triangular windows that arrange in a tetrahedral way around the cage centre.[21] In the solid state, CC3-R cages pack window-to-window, resulting in a 3-D interconnected diamondoid pore structure that runs through the centre of each cage. CC3-R crystals are stable to desolvation, giving rise to high levels of permanent microporosity with apparent Brunauer–

Emmett–Teller (BET) surface areas of up to 800 m^2g^{-1}, depending on the level of crystallinity.[41] Highly crystalline CC3-R has been shown to adsorb a variety of gases of different size and geometry, including hydrogen, nitrogen, methane, carbon dioxide, xenon, krypton and, most recently, sulfur hexafluoride.[1,19,41,42] All previous adsorption simulations on CC3-R adopted the standard GCMC method in conjunction with the rigid host model. This treatment has been shown to require fine-tuning of the host–guest interactions in order to reproduce the experimental adsorption isotherms.[1] Here, we combine the hybrid GCMC/MD scheme with some most widely used generic force fields to describe the host–guest interactions, thereby simulating the adsorption of CH_4, CO_2 and SF_6 in the fully flexible CC3-R. We show that experimental adsorption results can be reproduced correctly without altering the original force field parameters.

COMPUTATIONAL METHODOLOGIES

The molecular simulation software for adsorption and diffusion in flexible nanoporous materials, RASPA 2.0,[43] was used throughout this study. All hybrid GCMC/MD simulations included a hybrid MC/MD move, in which the MD path was computed in the isoenthalpic–isobaric (***NPH***) ensemble. Each MD move was performed for 5 timesteps of 0.5 fs each, with a probability of 2% in the simulation. The MD runs allowed the molecular cage crystals to relax upon the loading of the guest molecules, with newly relaxed configurations either accepted or rejected by the MC sampling rule.[44] Other trial MC moves included insertion, deletion, translation, rotation and reinsertion; these moves were randomly attempted with equal probabilities. All of the GCMC/MD and GCMC simulations involved an 800,000-cycle equilibration period followed by a 200,000-cycle production run; one cycle consisted of *n* MC moves, with *n* being equal to the number of adsorbate molecules (or 20, whichever is greater). In a typical GCMC/MD simulation performed here, the sampled MD path amounted to approximately 260 ps in total.

An accurate force field for the host structure is essential to account for the host flexibility correctly in GCMC/MD simulations. Recently, Holden *et al.* developed a bespoke force field, or the cage specific force field (CSFF), for a series of POC molecules including CC3-R.[31] CSFF was adopted to address the flexibility of CC3-R in our simulations. All force field parameters are given in Tables S3–S5, and RASPA force field definition files are also provided.

In our simulations, the non-bonding interatomic interactions—including host–host, guest–guest and host–guest pairs—were described using Lennard–Jones (LJ) interactions. 1–4 intramolecular non-bonding interactions were also turned on within the CC3-R cage molecule. Equation (**1**) was used to calculate the LJ interactions between host–host atom pairs in conjunction with the corresponding mixing rules by Equation (**2**), as used in CSFF. For host–guest and guest–guest atom pairs, the LJ interactions were calculated using Equation (**3**), with the Lorentz–Berthelot mixing rules by Equation (4).

$$E_{ij} = \varepsilon_{ij}[2(\frac{\sigma_{ij}}{r})^9 - 3.6(\frac{\sigma_{ij}}{r})^6] \quad (1)$$

$$\sigma_{ij} = [\frac{\sigma_i^6+\sigma_j^6}{2}]^{1/6}, \varepsilon_{ij} = \frac{2\sqrt{\varepsilon_i\varepsilon_j}\sigma_i^3\sigma_j^3}{\sigma_i^6\sigma_j^6} \quad (2)$$

$$E_{ij} = 4\varepsilon_{ij}[(\frac{\sigma_{ij}}{r})^{12} - (\frac{\sigma_{ij}}{r})^6] \quad (3)$$

$$\sigma_{ij} = \frac{\sigma_i+\sigma_j}{2}, \varepsilon_{ij} = \sqrt{\varepsilon_i\varepsilon_j} \quad (4)$$

where E_{ij} is the LJ potential between atoms *i* and *j*, separated by a distance *r*; σ_{ij} is the position at which the potential is zero; $\mathcal{E}_{ij}$ is the depth of the potential energy well. All LJ interactions were truncated at a cutoff distance of 12 Å. Three generic force fields, DREIDING,[45] OPLS,[46] and UFF[47], were used to assign LJ parameters to the host CC3 atoms when determining the intermolecular host–guest interactions with CH_4, CO_2 and SF_6. Electrostatic interactions were handled by the Ewald summation method with the relative precision set to 10^{-6}. Point charges of the atoms of CC3-

R were taken directly from CSFF, which were taken as the original PCFF charges derived by fitting to *ab initial* electrostatic potentials.[48] All non-bonded potential parameters are given in Table S6.

The LJ parameters of CH_4 and CO_2 were taken directly from the Transferable Potential for Phase Equilibria (TraPPE) force field.[49] The CH_4 molecule was treated as a united atom with the LJ parameters ε = 148 K, σ = 3.73 Å. The CO_2 molecule was modelled as a rigid, linear three-site molecule with atomic partial charges placed on each atom (O_CO_2: -0.35 e, C_CO_2: 0.7 e); its LJ parameters were assigned as ε = 79 K, σ = 3.05 Å for O_CO_2, and ε = 27 K, σ = 2.80 Å for C_CO_2. The SF_6 molecule was modelled atomistically and as rigid, with the LJ parameters ε = 163.89 K, σ = 3.246 Å for S, and ε = 27.24 K, σ = 2.954 Å for F, taken from the 7-site model by J. Samios *et al*.[50]

All simulation boxes contained one unit-cell of CC3-R with periodic boundary conditions exerted in three dimensions. Using CSFF, we first optimized the (empty) CC3-R crystal structure, starting with the experimentally reported, desolvated structure, using the Baker minimization method.[16,51] The final CSFF-optimized CC3-R crystal structure had a cubic cell with the cell length of 24.759 Å, in excellent agreement with the experimental cell length of 24.8 Å. Superimposing the optimized cage molecule on top of the experimental one revealed a similarity greater than 98%, with the average root-mean-square deviation of atomic positions being 0.2 Å (see Figure 1 and Table S2). We further calculated the pore size distribution (PSD) of the optimized CC3-R crystal structure, using the method from Gelb and Gubbins[52] as implemented in RASPA. As shown in Figure 2, there are two dominant pore sizes centred around 3.42 Å and 4.56 Å, which correspond to the interstitial cavity between two neighbouring cage molecules (marked 1 in Figure 2) and the cage cavity (marked 2 in Figure 2), respectively. These two key pore diameters of the CSFF-optimized CC3-R

are in good agreement with the values reported previously.[1] Hence, the CSFF implemented here was able to accurately model the molecular structure of CC3-R and its crystalline packing. The CSFF-optimized CC3-R crystal structure was used in all GCMC simulations (with the rigid host model) and as the starting host configuration in all GCMC/MD simulations.

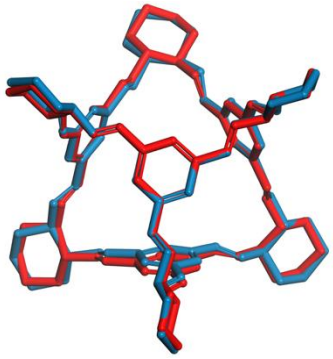

Figure 1. Overlay of CSFF-optimized (blue) and experimental (red) structures of the CC3-R molecule; hydrogen atoms were omitted for clarity.

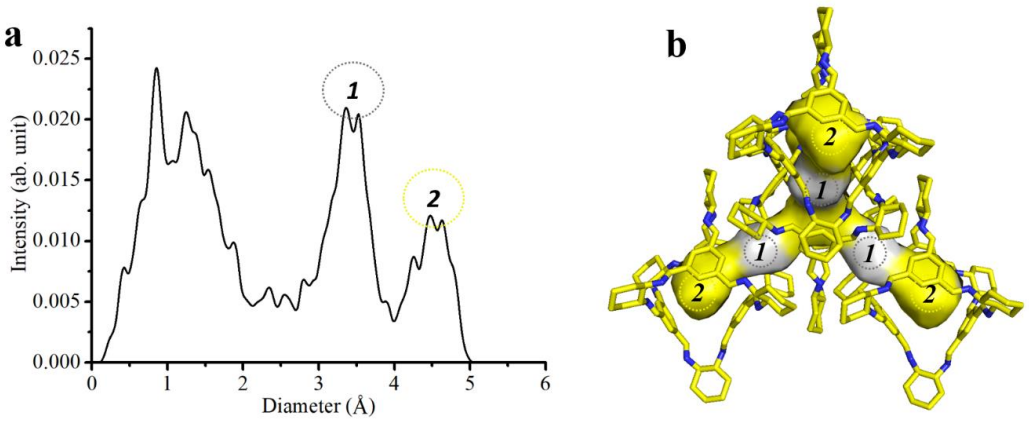

Figure 2. Pore size distribution (a) and the 3-D pore structure (b) of the CSFF-optimised crystal structure of CC3-R. The interstitial cavity between two adjacent cage windows is marked ***1*** and the cage cavity is marked ***2***.

RESULTS AND DISCUSSIONS

Adsorption isotherms of CH_4, CO_2 and SF_6 in CC3-R

Adsorption of CH_4, CO_2 and SF_6 in CC3-R was simulated with both the flexible and rigid host models to probe the effects of the CC3-R flexibility on its adsorption behaviours. Figure 3 summarizes all simulated adsorption isotherms, which are compared with their experimental counterparts.[16,42] For CH_4 adsorption (Figure 3a), DREIDING based simulations performed very well in reproducing the experimental isotherm, in terms of both the adsorption amounts and the shape of the isotherm, while the use of OPLS or UFF led to considerable overestimations. Interestingly, CH_4 isotherms predicted taking into account the flexibility of CC3-R do not differ significantly from those using a rigid host, which is the case for all three generic force fields tested. Similarly, Garcia-Sanchez *et al.* reported that the host flexibility had little influence on the CH_4 adsorption in LTA zeolites.[53] By contrast, CO_2 adsorption (Figure 3b) is sensitive to the treatment of CC3-R flexibility: the inclusion of host dynamics markedly enhances the uptake of CO_2, starting even from very low gas pressures, independent of the force-field choice for the host–guest interactions. For SF_6 (Figure 3c), the largest molecule amongst the three gases, it becomes essential to allow the host structure to fluctuate in order to accommodate the amounts of adsorbates measured experimentally, even for pressures as low as 0.038 bar. Clearly, the rigid CC3-R crystal structure has less than half of the pore space accessible to SF_6 in the flexible or experimental structure. It was also shown previously that the diffusion of SF_6 through CC3-R was facilitated by the dynamic nature of the cage structure. [42] Overall, the hybrid GCMC/MD simulations, using DREIDING based host–guest interactions, were able to reproduce the experimental adsorption isotherms for all the three gases. By contrast, all the other combinations between rigid-/flexible-host and DREIDING/OPLS/UFF were prone to overestimating the uptakes of the smaller CH_4 and CO_2 and severely underestimating those of the large SF_6.

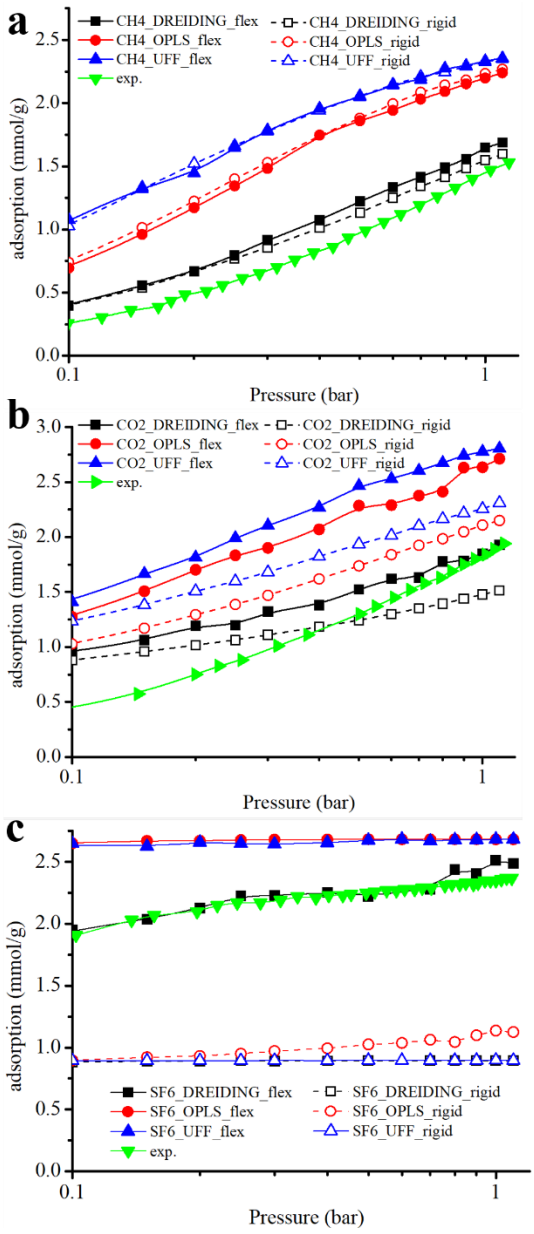

Figure 3. Predicted and experimental adsorption isotherms of CH_4 at 275 K (**a**), CO_2 at 289 K (**b**) and SF_6 at 273K(**c**) in CC3-R. The different host–guest force fields are colour-coded: black (squares), DREIDING; red (circles), OPLS; and blue (up-pointing triangles), UFF. Results based on the rigid host model and the flexible host model are indicated by unfilled symbols and filled symbols, respectively. Experimental results are shown as green, down-pointing triangles.

Adsorption positions of CH_4, CO_2 and SF_6 in CC3-R

To elucidate the effects of the structural flexibility of CC3-R on its adsorption of the different gases, we next focused on DREIDING based simulations with the rigid or flexible host model. Figure 4 shows an overly of simulation snapshots of CH_4, CO_2 and SF_6 molecules adsorbed in CC3-R at 1 bar. Simulations based on either the rigid or the flexible host model yielded similar adsorption locations of CH_4 and CO_2 in CC3-R. Both the interstitial cavities and the cage cavities (cavities ***1*** and ***2*** in Figure 2) are accessible to CH_4 and CO_2 molecules. The linear CO_2 molecules can additionally be adsorbed at the cage windows, which are too small for the spherical CH_4 molecules. Figure 4a–d also shows that the flexible CC3-R allows more CH_4 and CO_2 molecules to be accommodated in the pore structure, especially in the interstitial cavities and around the cage windows; both sites are the more confined spaces than the cage cavities in the rigid CC3-R. The influence of host flexibility becomes even more pronounced for SF_6 adsorption (Figure 4e,f). The interstitial cavities in the rigid CC3-R crystal structure are completely inaccessible to SF_6, though each cage cavity can adsorb one SF_6 molecule. By contrast, motions of the host atoms free up pore space for SF_6 adsorption in both the interstitial and the cage cavities. This explains the huge differences in the simulated SF_6 uptakes between the rigid and flexible host models shown in Figure 3c. In passing, we note that the SF_6 molecule located inside a rigid cage cavity is highly confined, whereas it can adopt more orientations when the cage is flexible.

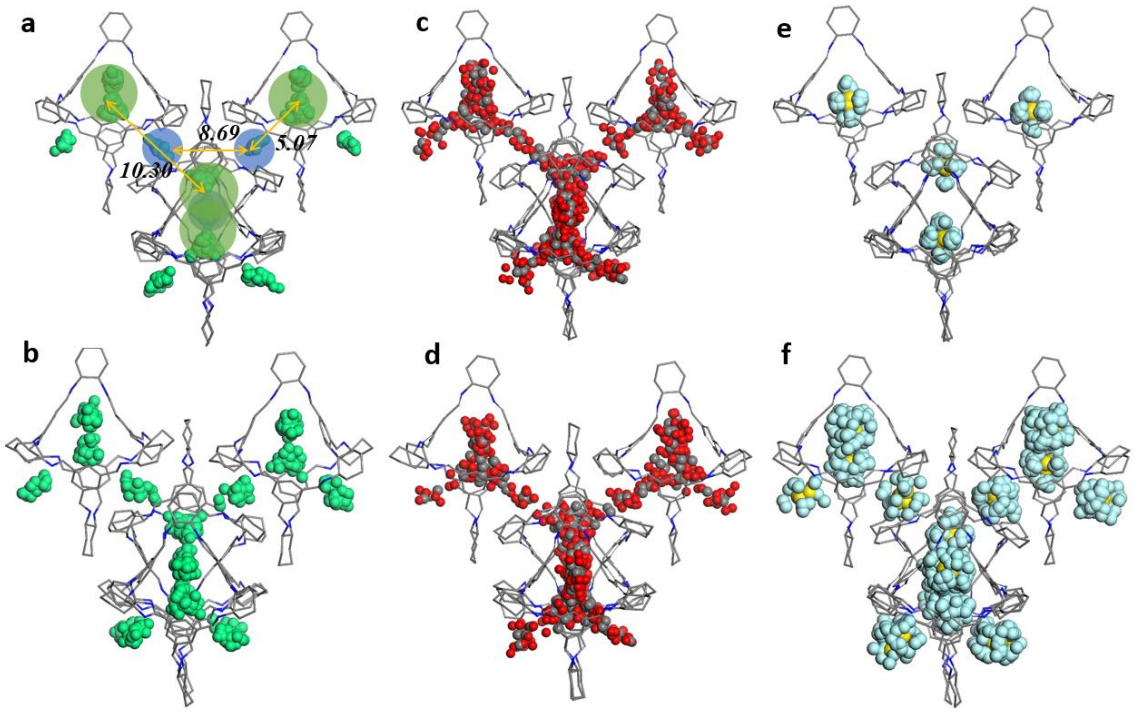

Figure 4. Overlay of thirty snapshots from the adsorption simulations of CH_4 (a, b; 275 K), CO_2 (c, d; 289 K), and SF_6 (e, f; 273 K) in CC3-R at 1 bar, based on the rigid host model (top) or the flexible host model (bottom): green, the united-atom representation of CH_4; grey and red, carbon and oxygen of CO_2, respectively; yellow and cyan, sulphur and fluorine of SF_6, respectively; hydrogen atoms of CC3-R are omitted for clarity, while carbon and nitrogen atoms are shown in grey and blue, respectively. The cage (green circles) and interstitial (blue circles) cavities are shown in (a); the centre-to-centre distances of cage–cage (*i.e.*, between two neighbouring cage cavities), cage–interstitial, and interstitial–interstitial cavities are 10.30, 5.07 Å, and 8.69 Å, respectively.

Radial distribution functions (RDFs) were used to characterize time-resolved conformational changes of each adsorbate molecule with respect to other adsorbate molecules (Figure 5). For CH_4 adsorption, the rigid host model and the flexible host model yielded the same characteristic CH_4–CH_4 distances, 5.18 Å and 8.87 Å (black curves in Figure 5), measured by the two distinct peaks of the RDFs for the pair. These distances correlate with the characteristic distance (5.07 Å) between

the centres of a cage cavity and one of its adjacent interstitial cavities and with that (8.69 Å) between the centres of two neighbouring interstitial cavities (see Figure 4a). In comparison, the SF_6–SF_6 RDFs show an additional peak at 11.00 or 11.20 Å, with the flexible or rigid host model, respectively. This corresponds to the characteristic distance (10.30 Å) between the centres of two neighbouring cage cavities. The narrower, sharper peaks in the SF_6–SF_6 RDF (flexible host), compared to those of the CH_4–CH_4 counterpart, indicate that the SF_6 molecules are more confined to the specific adsorption sites than the smaller CH_4 molecules. Again, not surprisingly, the SF_6–SF_6 RDF of the rigid host model only shows characteristic distances for SF_6 adsorbed inside different cage cavities, corroborating the simulation snapshots shown in Figure 4e. The CO_2–CO_2 RDFs show a different picture: the adsorbed CO_2 molecules pack densely in CC3-R, with their close proximity indicated by a single, distinct RDF peak at 4.08 Å.

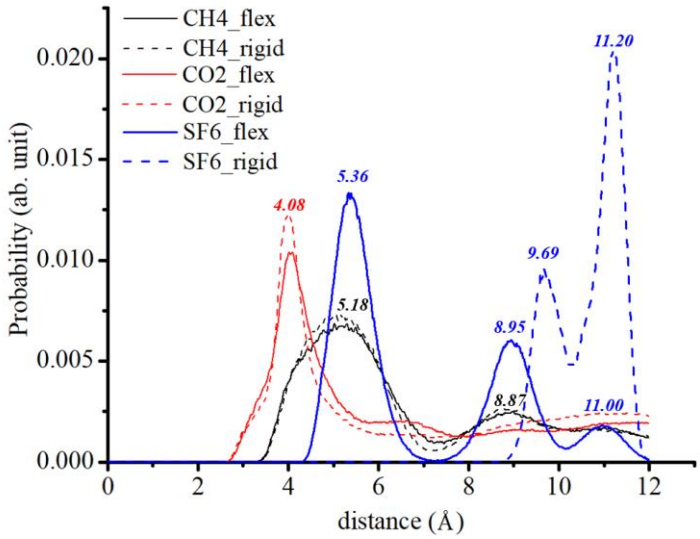

Figure 5. Radial distribution functions computed for CH_4–CH_4 (black; 275 K), CO_2–CO_2 (red; 289 K), and SF_6–SF_6 (blue; 273 K) during the adsorption simulations with the flexible host model (solid curves) or the rigid host model (dashed curves), all at 1 bar.

Structural dynamics of CC3-R loaded with CH_4, CO_2 and SF_6

We monitored pore-size changes in the flexible CC3-R loaded with CH_4, CO_2 or SF_6 at 1 bar and at the same temperatures explored above. For each system, we calculated PSD for thirty snapshots taken from the production run of the hybrid GCMC/MD simulation, after deleting all the guest molecules in the structure. For comparison, we performed MD simulations for the empty CC3-R crystal structure at the respective temperatures and calculated PSD histograms in the same way as for the guest-loaded systems. Figure 6 shows overlays of such snapshots for the three gases, together with the PSD of the static crystal structure of CC3-R. The adsorption of CH_4 did not result in marked changes in the sizes of the interstitial or cage cavities (Figure 6b). Similarly, the CO_2 adsorption did not change the crystal structure of CC3-R drastically, but still the pore-size increases in both types of cavities were noticeable (Figure 6c). The broader, flatter PSD profiles of CO_2-loaded CC3-R indicate that the CC3-R structure was expanded more uniformly by taking up CO_2 than CH_4. More significantly, the largest guest molecule amongst the three, SF6, expanded the host structure considerably, with the interstitial and cage cavities enlarged by approx. 0.73 Å and 0.67 Å, respectively. Accordingly, the available pore volume of CC3-R was increased most upon the adsorption of SF_6, compared to the other two gases (Figure S7). The fact that pore sizes in CC3-R vary depending on the adsorbate's identity suggests a cooperative adsorption mechanism in action: the host flexibility is required to facilitate guest adsorption, which in turn influences the host structure and its dynamics. The phenomenon of cooperativity is very challenging to explore by experiment, so here simulations may offer a unique insight.

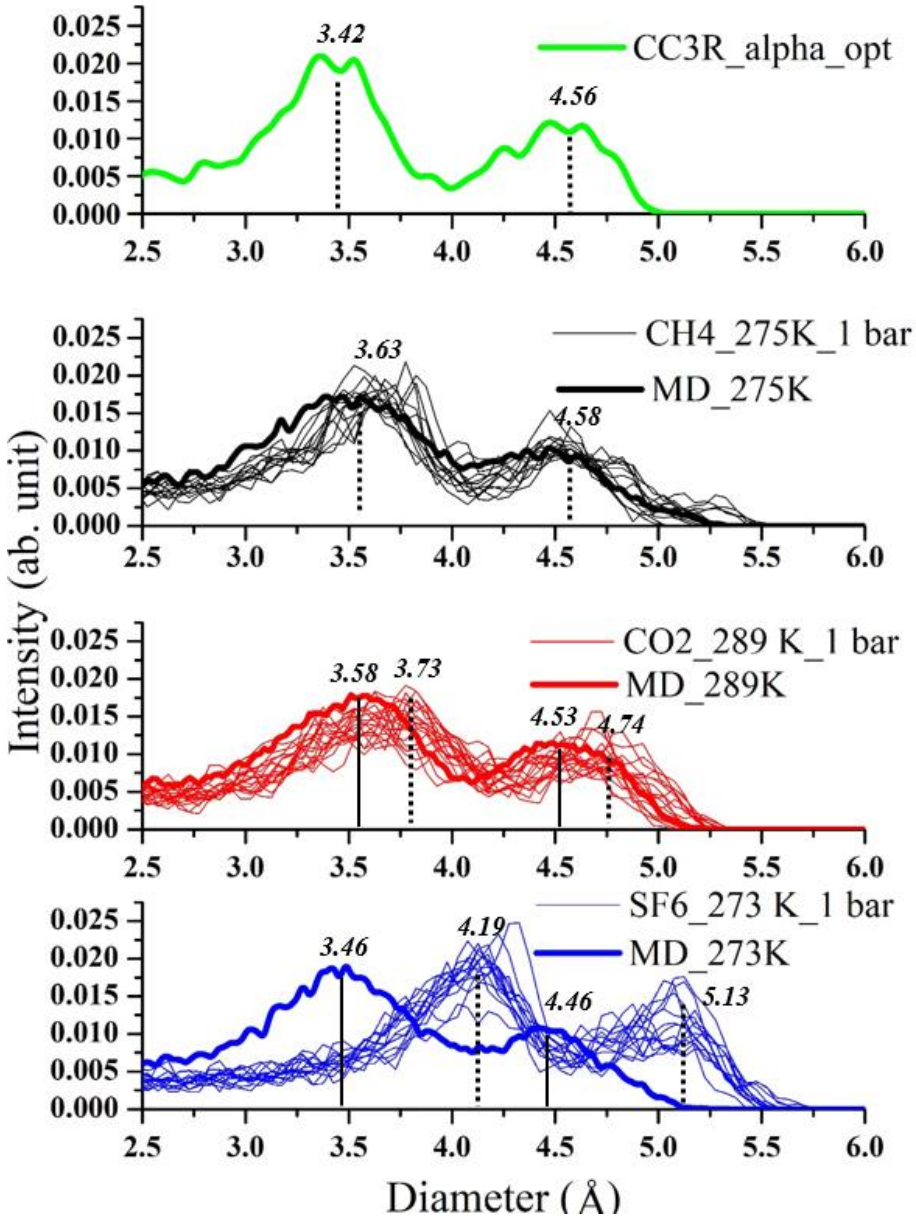

Figure 6, Pore size distribution (PSD) of the CSFF-optimized, static CC3-R with zero loading (a) and overlay of PSDs of thirty snapshots taken from the hybrid GCMC/MD simulations of CC3-R loaded CH_4 (b; 275 K), CO_2 (c; 289 K), or SF_6 (d; 273 K), and blank host MD simulations all at 1 bar.

CONCLUSIONS

This study shows that the structural flexibility of the porous molecular crystal CC3-R must be taken into account to adequately describe the adsorption of SF_6 and, by analogy, other large guest molecules. On the other hand, the adsorption of small gases, such as CH_4 and CO_2, can be predicted reasonably well with the rigid host structure, requiring significantly less computational effort. More generally, we demonstrate that hybrid GCMC/MD simulations are a powerful approach for directly probing gas adsorption in flexible hosts, thus allowing for improved understanding of dynamic and cooperative adsorption events.

ASSOCIATED CONTENT

Supporting Information. Force field parameters, point charges, and additional computational data.

AUTHOR INFORMATION

Corresponding Author: Lifeng Ding (Lifeng.Ding@xjtlu.edu.cn); Linjiang Chen (Linjiang.Chen@liverpool.ac.uk)

ACKNOWLEDGMENTS

The authors acknowledge financial support from the Chinese Young Scholar National Science Foundation Grant (21403171), the Xi'an JiaoTong-Liverpool University (XJTLU) Research Development Fund (PGRS-13-03-08), and the Key Program Special Fund in XJTLU (KSF-E-03). The authors acknowledge utilization of the computational resources from the Shenzhen Cloud Computing Center. The work was also supported by the Engineering and Physical Sciences Research Council (EPSRC) (EP/N004884/1) and the Leverhulme Trust via the Leverhulme Research Centre for Functional Materials Design.

REFERENCES

1. Chen, L. *et al.* Separation of rare gases and chiral molecules by selective binding in porous organic cages. *Nat. Mater.* **13,** 954–60 (2014).

2. Holden, D. *et al.* Understanding Static, Dynamic and Cooperative Porosity in Molecular Materials. *Chem. Sci.* **00,** 1–5 (2016).

3. Barbour, L. J. Crystal porosity and the burden of proof. *Chem. Commun.* 1163 (2006). doi:10.1039/b515612m

4. Cheetham, A. K., Férey, G. & Loiseau, T. Open-Framework Inorganic Materials. *Angew. Chemie Int. Ed.* **38,** 3268–3292 (1999).

5. Kitagawa, S., Kitaura, R. & Noro, S. Functional porous coordination polymers. *Angew. Chemie - Int. Ed.* **43,** 2334–2375 (2004).

6. Yaghi, O. M. *et al.* Reticular synthesis and the design of new materials. *Nature* **423,** 705–714 (2003).

7. Cote, A. P. Benin, A. I. Ockwig, N. W. O'Keeffe, M. Matzger, A. J. Yaghi, O. M. Porous, Crystalline, Covalent Organic Frameworks. *Science (80-.).* **310,** 1166–1170 (2005).

8. Park, K. S. *et al.* Exceptional chemical and thermal stability of zeolitic imidazolate frameworks. *Proc. Natl. Acad. Sci. U. S. A.* **103,** 10186–10191 (2006).

9. Ben, T. *et al.* Targeted Synthesis of a Porous Aromatic Framework with High Stability and Exceptionally High Surface Area. *Angew. Chemie* **121,** 9621–9624 (2009).

10. Mastalerz, M. Shape-persistent organic cage compounds by dynamic covalent bond formation. *Angew. Chemie - Int. Ed.* **49,** 5042–5053 (2010).

11. Holst, J. R., Trewin, A. & Cooper, A. I. Porous organic molecules. *Nat. Chem.* **2,** 915–920 (2010).

12. Tian, J., Thallapally, P. K. & McGrail, B. P. Porous organic molecular materials. *CrystEngComm* **14,** 1909 (2012).

13. Hasell, T., Chong, S. Y., Schmidtmann, M., Adams, D. J. & Cooper, A. I. Porous organic alloys. *Angew. Chemie - Int. Ed.* **51,** 7154–7157 (2012).

14. McKeown, N. B. Nanoporous molecular crystals. *J. Mater. Chem.* **20,** 10588 (2010).

15. Dalgarno, S. J., Thallapally, P. K., Barbour, L. J. & Atwood, J. L. Engineering void space in organic van der Waals crystals: calixarenes lead the way. *Chem. Soc. Rev.* **36,** 236–245 (2007).

16. Tozawa, T. *et al.* Porous organic cages. *Nat. Mater.* **8,** 973–978 (2009).

17. Jones, J. T. a. *et al.* On-Off Porosity Switching in a Molecular Organic Solid. *Angew. Chemie Int. Ed.* **50,** 749–753 (2011).

18. Kewley, A. *et al.* Porous Organic Cages for Gas Chromatography Separations. *Chem. Mater.* **27,** 3207–3210 (2015).

19. Mitra, T. *et al.* A soft porous organic cage crystal with complex gas sorption behavior. *Chem. - A Eur. J.* **17,** 10235–10240 (2011).

20. Krishna, R. & van Baten, J. M. In silico screening of metal-organic frameworks in separation applications. *Phys. Chem. Chem. Phys.* **13,** 10593–10616 (2011).

21. Holden, D. *et al.* Gas Diffusion in a Porous Organic Cage: Analysis of Dynamic Pore Connectivity Using Molecular Dynamics Simulations. *J. Phys. Chem. C* **118,** 12734–12743 (2014).

22. Babarao, R., Dai, S. & Jiang, D. E. Functionalizing porous aromatic frameworks with polar organic groups for high-capacity and selective CO 2 separation: A molecular simulation study. *Langmuir* **27,** 3451–3460 (2011).

23. Smit, B. & Krishna, R. Monte Carlo simulations in zeolites. *Curr. Opin. Solid State Mater. Sci.* **5,** 455–461 (2001).

24. Düren, T., Bae, Y.-S. & Snurr, R. Q. Using molecular simulation to characterise metal–organic frameworks for adsorption applications. *Chem. Soc. Rev.* **38,** 1237 (2009).

25. Krishna, R. Diffusion in porous crystalline materials. *Chem. Soc. Rev.* **41,** 3099 (2012).

26. Pulido, A. *et al.* Functional materials discovery using energy-structure-function maps. *Nature* **543,** 657–664 (2017).

27. Liu, Y. *et al.* Reversible structural transition in MIL-53 with large temperature hysteresis. *J. Am. Chem. Soc.* **130,** 11813–11818 (2008).

28. Jones, J. T. A. *et al.* On-off porosity switching in a molecular organic solid. *Angew. Chemie - Int. Ed.* **50,** 749–753 (2011).

29. Andreetti, G. D., Ungaro, R. & Pochini, A. Crystal and Molecular Structure of Cyclo{quater[(5-t-butyl-2-hydroxy-1,3- pheny1ene)methylenel) Toluene (1 : 1) Clathrate. *J. Chem. Soc. Chem. Commun.* 1005–1007 (1979).

30. Chen, L. *et al.* Separation of rare gases and chiral molecules by selective binding in porous organic cages. *Nat Mater* **13,** 954–960 (2014).

31. Holden, D., Jelfs, K. E., Cooper, A. I., Trewin, A. & Willock, D. J. Bespoke force field for simulating the molecular dynamics of porous organic cages. *J. Phys. Chem. C* **116,** 16639–16651 (2012).

32. Salles, F. *et al.* Molecular insight into the adsorption and diffusion of water in the versatile hydrophilic/hydrophobic flexible MIL-53(Cr) MOF. *J. Phys. Chem. C* **115,** 10764–10776 (2011).

33. Chokbunpiam, T. *et al.* The importance of lattice flexibility for the migration of ethane in ZIF-8: Molecular dynamics simulations. *Microporous Mesoporous Mater.* **174,** 126–134 (2013).

34. Vlugt, T. J. H. Influence of Framework Flexibility on the Adsorption Properties of Hydrocarbons in the Zeolite Silicalite. 12757–12763 (2002).

35. Gee, J. A. & Sholl, D. S. Effect of Framework Flexibility on C8 Aromatic Adsorption at High Loadings in Metal-Organic Frameworks. *J. Phys. Chem. C* **120,** 370–376 (2016).

36. Wu, W. P. *et al.* Double-step CO sorption and guest-induced single-crystal-to-single-crystal transformation in a flexible porous framework. *Dalt. Trans.* **44,** 10141–10145 (2015).

37. Meza-Morales, P. J. *et al.* CO_2 adsorption-induced structural changes in coordination polymer ligands elucidated via molecular simulations and experiments. *Dalt. Trans.* **45,** 17168–17178 (2016).

38. Shi, Y. X., Li, W. X., Zhang, W. H. & Lang, J. P. Guest-Induced Switchable Breathing Behavior in a Flexible Metal-Organic Framework with Pronounced Negative Gas Pressure. *Inorg. Chem.* **57,** 8627–8633 (2018).

39. Sheng, Y. *et al.* Guest-Induced Breathing Effect in a Flexible Molecular Crystal. *Angew. Chemie - Int. Ed.* **55,** 3378–3381 (2016).

40. Nikolayenko, V. I., Castell, D. C., van Heerden, D. P. & Barbour, L. J. Guest-Induced Structural Transformations in a Porous Halogen-Bonded Framework. *Angew. Chemie -*

Int. Ed. **57,** 12086–12091 (2018).

41. Hasell, T., Chong, S. Y., Jelfs, K. E., Adams, D. J. & Cooper, A. I. Porous organic cage nanocrystals by solution mixing. *J. Am. Chem. Soc.* **134,** 588–598 (2012).

42. Hasell, T. *et al.* Porous organic cages for sulfur hexafluoride separation. *J. Am. Chem. Soc.* (2016). doi:10.1021/jacs.5b11797

43. Dubbeldam, D., Calero, S., Ellis, D. E. & Snurr, R. Q. RASPA: molecular simulation software for adsorption and diffusion in flexible nanoporous materials. *Mol. Simul.* **7022,** 1–21 (2015).

44. Gilks, W. R., Best, N. G. & Tan, K. K. C. Adaptive Rejection Metropolis Sampling within Gibbs Sampling. *Appl. Stat.* **44,** 455 (1995).

45. Mayo, S. L., Olafson, B. D., Iii, W. a G., Eb, E. & El, E. a E. T. DREIDING: A Generic Force Field for Molecular Simulations. *J. Phys. Chem.* **101,** 8897–8909 (1990).

46. Jorgensen, W. L. *et al.* Development and Testing of the OLPS All-Atom Force Field on Conformational Energetics and Properties of Organic Liquids. *J. Am. Chem. Soc.* **118,** 11225–11236 (1996).

47. Simulations, M. D. UFF, a Full Periodic Table Force Field for Molecular Mechanics and Molecular Dynamics Simulations. *J. Am. Chem. Soc.* **114,** 10024–10035 (1992).

48. Sun, H. Ab Initio Calculations and Force Field Development for Computer Simulation of Polysilanes. *Macromolecules* **28,** 701–712 (1995).

49. Martin, M. G. & Siepmann, J. I. Transferable Potentials for Phase Equilibria. 1. United-Atom Description of n -Alkanes. *J. Phys. Chem. B* **102,** 2569–2577 (1998).

50. Dellis, D. & Samios, J. Molecular force field investigation for Sulfur Hexafluoride: A

computer simulation study. *Fluid Phase Equilib.* **291,** 81–89 (2010).

51. Baker, J. An algorithm for the location of transition states. *J. Comput. Chem.* **7,** 385–395 (1986).

52. Gelb, L. D. & Gubbins, K. E. Pore Size Distributions in Porous Glasses: A Computer Simulation Study. *Langmuir* **15,** 305–308 (1999).

53. García-Sánchez, A., Dubbeldam, D. & Calero, S. Modeling adsorption and self-diffusion of methane in LTA zeolites: The influence of framework flexibility. *J. Phys. Chem. C* **114,** 15068–15074 (2010).